arXiv:1403.5091v1 [physics.atom-ph] 20 Mar 2014

Charge Exchange Collisions between Ultracold Fermionic Lithium Atoms and Calcium Ions

Shinsuke Haze, Munekazu Fujinaga, Ryoichi Saito and Takashi Mukaiyama
Institute for Laser Science, University of Electro-Communications,
1-5-1 Chofugaoka, Chofu, Tokyo 182-8585, Japan

An observation of charge exchange collisions between ultracold fermionic ^{6}Li atoms and $^{40}Ca^+$ ions is reported. The reaction product of the charge exchange collision is identified via mass spectrometry where the motion of the ions is excited parametrically. We measure the cross section of the charge exchange collisions between the ^{6}Li atoms in the ground state and the $^{40}Ca^+$ ions in the ground and metastable excited states. Investigation of the inelastic collision characteristics in the atom-ion mixture is an important step toward ultracold chemistry based on ultracold atoms and ions.

PACS numbers: 37.10.Ty,03.67.Lx

The chemical properties of particles at low temperatures are expected to be quite different from those at high temperatures. At high temperatures, a chemical reaction rate is determined by the probability to cross over an energy barrier between the reactant and the product due to thermal fluctuation. However, at low temperatures where the wave nature of a particle plays an important role in a chemical reaction, the tunneling of the energy barrier affects the reaction and the reaction rate. In such a situation, the reaction rate would be strongly modified from the classical prediction. For extremely low temperatures, the quantum statistics of particles influences the chemical reaction, and bosonic enhancement [1] or suppression due to Fermi statistics in a chemical reaction is expected to be observed.

A hybrid system of ultracold atoms and ions offers an ideal platform to study ultracold chemical reactions, since sophisticated techniques to efficiently cool and detect atoms and ions have been developed. Elastic and inelastic collision cross sections between ultracold atoms and ions have been successfully determined in various atom-ion combinations [2–9]. Recently, a charge exchange collision, which is one of the elementary processes in chemical reactions, was observed at a single particle level using a trapped $^{174}Yb^+$ ion immersed in a Bose-Einstein condensate of ^{87}Rb atoms [7]. In order to experimentally observe the emergence of a quantum statistical nature in a chemical reaction in an atom-ion hybrid system, it is necessary to go into an ultralow temperature regime where only a few partial waves contribute to the atom-ion interactions.

A typical energy scale of the threshold for the quantum collision regime is given by $E_{\rm th} = \hbar^4/2C_4\mu^2$, where $\mu = m_{\rm i}m_{\rm a}/(m_{\rm i}+m_{\rm a})$ is the reduced mass of an atom of mass $m_{\rm a}$ and an ion of mass $m_{\rm i}$, and $C_4 = \alpha Q^2/4\pi\epsilon_0$, where α, Q, and ϵ_0 are the atomic polarizability, the charge of the ion, and the vacuum permittivity, respectively. As clearly shown in the expression of $E_{\rm th}$, choosing an atom-ion combination with a small reduced mass is advantageous to reach the quantum collision regime. In addition, recent theoretical research revealed that the heating effect in an atom-ion hybrid system caused by an ion micromotion, which is a rapidly driven motion in a Paul trap, can be minimized by also using a small $m_{\rm a}/m_{\rm i}$ ratio [12]. Considering these properties, using Li atoms for a neutral species would be a preferable choice of atom-ion combinations for the study of ultracold quantum chemistry.

In this article, we report an observation of the charge exchange collisions in a mixture of ^{6}Li atoms and $^{40}Ca^+$ ions. The loss of ions due to inelastic collisions between the ^{6}Li atoms in the ground hyperfine state and ions in both the ground state ($S_{1/2}$) and excited states ($D_{3/2}$ and $D_{5/2}$) is observed. We ascertain that the inelastic collision is a charge exchange collision by identifying the collision product to be Li^+ ions via the mass spectrometry with parametric excitation. Since the reduced mass of the Li-Ca^+ combination is relatively small compared to that of the other recently realized combinations, the system has a higher $E_{\rm th}$ and a smaller heating rate due to micromotion. The calculated $E_{\rm th}$ for the ^{6}Li-$^{40}Ca^+$ mixture is $k_{\rm B}\times 10\mu$K, which is much higher than $k_{\rm B}\times$ 44 nK for ^{87}Rb-$^{138}Ba^+$ [5], $k_{\rm B}\times$ 53 nK for ^{87}Rb-$^{174}Yb^+$ [4], and $k_{\rm B}\times$ 280 nK for ^{40}Ca-$^{174}Yb^+$ [6]. The heating rate

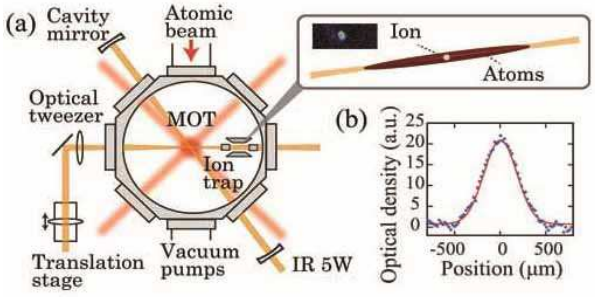

FIG. 1: (a) Schematic drawing of the experimental setup. A single ion is trapped in a linear Paul trap and immersed in a gas of fermionic atoms in an optical dipole trap. Atoms are transported with an optical tweezer following a cavity-enhanced optical dipole trap. (b) A typical one-dimensional density profile of a Fermi gas after a 2 msec expansion fitted by a Thomas-Fermi distribution with $T/T_{\rm F}$=0.94.

calculated based on the model by Cetina et al. [12] for the Li-Ca^+ combination is 0.5 μK/sec, which is roughly two orders of magnitude smaller than those for other currently realized combinations, and small enough to keep the system in the quantum collision regime for a reasonable timescale for the experiments. Along with this advantage, our atom-ion mixture is expected to be applicable for novel Fermi gas experiments where the ion can be introduced as a probe head localized in a sub-micron spatial region [10] or a single charged impurity acting as a polaronic excitation in Fermi condensates [11].

In our experiment, Ca^+ ions and ^{6}Li atoms are prepared at different positions in the trap chamber and mixed with each other after all the cooling processes are complete. Figure 1(a) schematically shows the experimental setup. Ca^+ ions are trapped and doppler-cooled with the $S_{1/2}$-$P_{1/2}$ transition in a linear Paul trap composed of four RF electrodes and two endcaps, which are located 5 cm away from the center of the trap chamber [9]. The ion trap is driven with a 2.9 MHz RF field and the trap frequencies of the Ca^+ ions are $(\omega_r, \omega_z) = 2\pi\times(170,\ 35)$ kHz, where ω_r and ω_z denote the radial and axial trapping frequencies, respectively. The fluorescence from the ions is collected onto a photo-multiplier tube (PMT) and a charge-coupled-device (CCD) camera. ^{6}Li atoms are captured in a magneto-optical trap and transferred into an optical trap, which has a relatively large trap volume and a deep trap depth ($\sim$1 mK) that is created by an enhanced light field by using an optical resonator [13, 14]. Subsequently, the atoms are transferred into a tightly-focused dipole trap and further cooled to a quantum degenerated regime via evaporative cooling. During evaporative cooling, the optical potential is reduced in 6 sec at the 300 Gauss bias magnetic field. After evaporation, the atoms are transported to the location of the ion trap electrodes by translating the focusing lens of the trap laser and mixed with ions. The final temperature of the atomic gas is 900 nK and the corresponding ratio of the atomic to Fermi temperature is T/T_F=0.94, which are determined by fitting the density profile with the Thomas-Fermi distribution (Fig. 1(b)).

In order to observe the inelastic collisions between the atoms and ions, several to ten ions are initially loaded into an ion trap, and just before overlapping them with atoms, the ions are pumped to either the $S_{1/2}$, $D_{3/2}$, or $D_{5/2}$ state. To pump the ions to the $D_{3/2}$ ($D_{5/2}$) state, the ions are illuminated by 397 nm (397 nm and 850 nm) lasers for 20 msec after the doppler cooling. To prepare the ions in the $S_{1/2}$ state, the 866 nm laser is kept on for 20 msec after the cooling. The ^{6}Li atoms are prepared in the lowest spin states of $S_{1/2}$ ($|\ F = 1/2, m_F = \pm 1/2\rangle$) with an even population. For the measurement of the inelastic collisions, the evaporative cooling is applied until the atomic temperature is 50 μK and the number of atoms is 8×10^4. The radial and axial trapping frequencies of the optical dipole trap are 5.9 kHz and 39 Hz, respectively.

Figures 2(a) and 2(b) show the fluorescence images of the ions before and after undergoing an inelastic collision, which causes the ion fluorescence from one of the ions to completely diminish. Considering that the ion position shifted after the inelastic collision, the product of the inelastic collision is lost from the ion trap. Figure 2(d) shows the relationship between the ion detection probability and interaction time. The black, red, and blue markers show the data taken for the ions in the $S_{1/2}$, $D_{3/2}$, and $D_{5/2}$ states before the atom-ion interaction, and the data are averaged over 40 to 100 measurements. Although the ions in the $S_{1/2}$ state are stable against the inelastic collisions, the ions in the $D_{3/2}$ and $D_{5/2}$ states experience inelastic collisions at a finite rate.

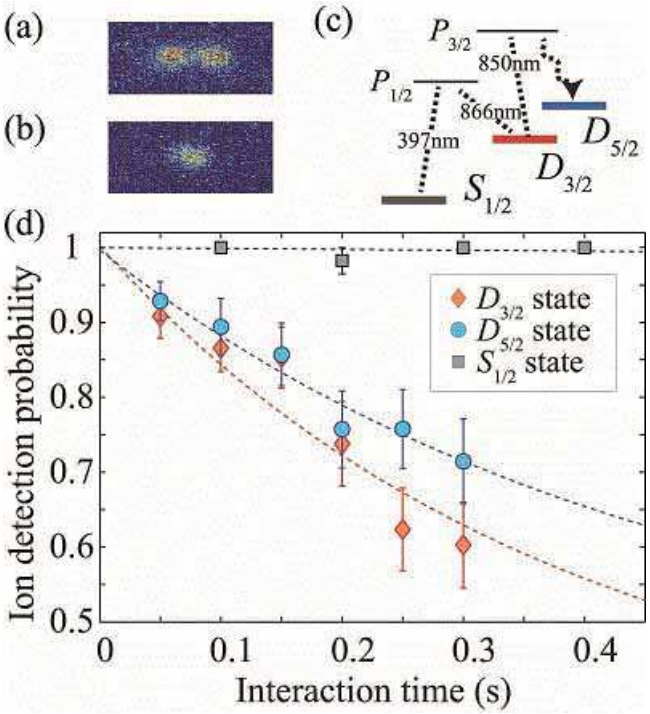

FIG. 2: Fluorescence images of the ions (a) before and (b) after undergoing an inelastic collision. (c) The relevant levels of $^{40}Ca^+$. (d) The relationship between the ion detection probability and interaction time.

The ion detection probability in the D states can be analyzed using rate equations. With the probabilities of finding the ions in the S, D, and final states after the two-body inelastic collision (p_S, p_D, $p_{\rm inel}$, respectively), the rate equations can be written as $\dot{p}_D = -\Gamma p_D - \gamma p_D$, $\dot{p}_S = \gamma p_D$, and $\dot{p}_{\rm inel} = \Gamma p_D$, and $p_S + p_D + p_{\rm inel} = 1$ must be satisfied, where γ is the radiative decay rate of the D state, and Γ is the inelastic collision rate that is the objective in this experiment. The spontaneous decay rate γ was precisely measured to be 0.86 (0.85) Hz for $D_{5/2}$ ($D_{3/2}$) in a previous study [16]. The dashed curves shown in Fig. 2(c) are the fitting results that are obtained by using the solution of the rate equations with Γ as a fitting parameter. Here, the initial conditions of the rate equation are $p_D(0) = 1$, $p_S(0) = 0$, and

$p_{\rm inel}(0) = 0$. The obtained values of Γ from the fitting are $(\Gamma_{D_{3/2}}, \Gamma_{D_{5/2}}) = (1.79(14),\ 1.30(5))$ Hz, and Γ_S is measured to be less than 1.2×10^{-2} Hz. The corresponding loss coefficient $K = \frac{\Gamma}{n_{\rm a}}$ can be determined from the atomic density $n_{\rm a}$ [15], and the coefficients are obtained to be $(K_{D_{3/2}}, K_{D_{5/2}})=(8.2 \times 10^{-17},\ 5.9 \times 10^{-17})$ m^3/sec and $K_{S_{1/2}}$ is obtained to be smaller than 7.1×10^{-19} m^3/sec. Since $K_{D_{3/2}}$ and $K_{D_{5/2}}$ are smaller than the Langevin collision coefficient $K_{\rm L} = 5.0 \times 10^{-15}$ m^3/sec [17] by roughly two orders of magnitude, and $K_{S_{1/2}}$ is smaller by four orders of magnitude, the inelastic collision is essentially a off-resonant process, which shows a clear contrast to the case of homonuclear combinations [3].

The inelastic collision can either be a charge exchange collision or collisional quenching from the metastable D state to the ground state. However, the expected recoil energy of the Ca^+ ions as a result of the collisional quenching from the $D_{3/2}$ and $D_{5/2}$ states is 0.24 eV, which is four times smaller than the trap depth in the current setup. Therefore, we consider that the inelastic collision observed in this study is dominantly a charge exchange collision. For the measurement explained above, the amplitude and frequency of the RF field are chosen such that $q_{\rm Ca^+}$=0.16 and $q_{\rm Li^+}$=1.2, where the q-parameter is $q = \frac{2Q^2 U_{\rm rf}}{m_i r_0^2 \Omega_{\rm rf}^2}$ [18] with $\Omega_{\rm rf}$, $U_{\rm rf}$, and r_0 as the frequency and amplitude of the applied RF field, and the separation between the ion and the electrodes, respectively. These parameters are chosen not to keep the Li^+ ions, which is the reaction product of the charge exchange process, in the Paul trap. This is done because Ca^+ would be heated by the collisions with the remaining Li^+ ions, which would cause the Ca^+ ion images for the ion number counting to be blurred.

We then measure the atomic-density dependence of the ion loss rate. The ions are moved inside the atomic cloud and the effective atomic density for the ion to overlap is controlled. To change the position of an ion in the radial direction, DC voltage is applied to one of the ion trap electrodes. A displacement in an axial direction is applied by changing the travel distance of the focusing lens for the optical tweezer. The relationships between the measured loss rate and the atom-ion displacement in the radial and axial directions are plotted in Figs. 3(a) and 3(b). The calculated radial size of the atoms and ions are $r_{\rm rad}$=10 μm and $r_{\rm ion}$=45 μm, respectively. The position dependence of the inelastic collision reflects the overlap integral of the density profiles of the atoms and ions. The 1/e width derived from the Gaussian fitting to the data in Figs. 3(a) is 46(4)μm, which is consistent with the predicted value of $\sqrt{r_{\rm ion}^2 + r_{\rm rad}^2} = 46\mu$m. Figure 3(b) shows the relationship between the inelastic collision rate and displacement of the ion in the axial direction. The 1/e width of the profile is 2.0(4) mm, which is consistent with the size of the atomic cloud in the axial direction. Figure 3(c) shows the ion loss rate as a function of the average atomic density [15]. We find that the

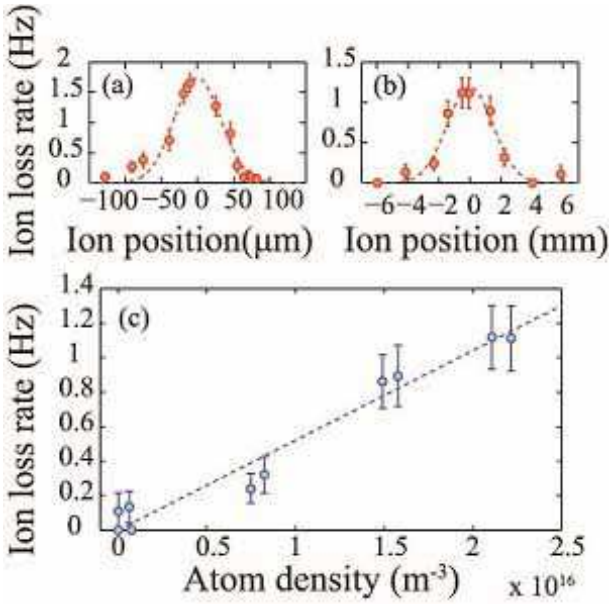

FIG. 3: Measured (a) radial and (b) axial overlap profile of the atoms and a single ion. (c) The ion loss rate is plotted against the atomic density. The dashed line is the fitting result with a linear function.

ion loss rate linearly increases as the atomic density increases, suggesting that the inelastic collisions observed in this experiment are atom-ion two-body processes.

In order to identify the reaction product unambiguously, the amplitude and the frequency of the RF field is changed to set $q_{\rm Li^+}$=0.50, which is within the stability region of an ion trap [18]. With this condition, we are able to keep the Li^+ ions in the trap and perform the well-established mass spectrometry demonstrated in [5, 19, 20]. A pure Ca^+ ion cloud consisting of ∼400 ions is mixed with atoms for 4 sec and the Li^+ ions are then created in the charge exchange process. Subsequently, an oscillating electric field is applied to one of the electrodes of the ion trap to excite the radial motion of the ions. The fluorescence from the Ca^+ ions is detected by the PMT and the photon counts are recorded while we sweep the frequency of the applied oscillating field.

The experimental results of the mass spectrometry are shown in Fig. 4(a). The blue and red dots show the fluorescence from the ions, before(red) and after(blue) mixing the ions with the atoms, as a function of the frequency of the applied oscillating field. The blue dots show a reduction in the fluorescence of the ions that peaked at 1020 kHz, which is an indication of the resonant motional excitation of the Li^+ ions. The vertical dashed line at 966 kHz indicates the expected resonance frequency of the Li^+ ions, which is calculated from the measurement of the resonant radial frequency of the Ca^+ ions observed at 145 kHz. The shaded bar indicates the uncertainty of the resonance peak, which is originated from the consideration of the spectral broadening of the measured resonance signal of the Ca^+ ions. The slight

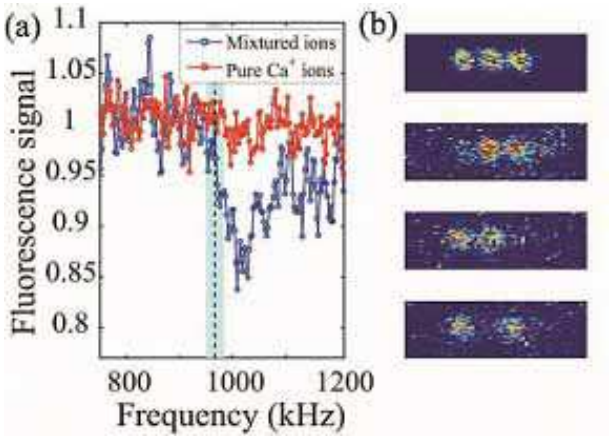

FIG. 4: (a) The mass spectrometry results of the ions in the trap. The vertical axis is the normalized fluorescence from the Ca^+ ions and the horizontal axis is the frequency of the applied oscillating field. The reduction of the ion fluorescence indicates the existence of the Li^+ ions in the trap. (b) Fluorescence images of the ions before (top panel) and (lower three panels) after atom-ion interaction. The images in the lower three panels are taken at different times. A dark ion moving in the ion crystal is detected.

discrepancy of the resonant frequency of 5 % is due to a Coulomb-interaction induced shift in the mass spectrometry of multispecies ion crystals [21]. We have also performed the same measurement around the resonant frequency of $CaLi^+$ and Li_2^+ molecular ions, however, no resonant excitation signal is observed.

The significant differences between the charge exchange collision coefficients for the S and D states may originate from the existence of the closely lying energy levels Li^++Ca(3d4s ^3D) for the D states. A similar behavior was observed in the Rb-Yb^+ experiment, where the reaction rates of the ions with the metastable $D_{3/2}$ and $F_{7/2}$ states were investigated in detail [7]. We assume that one of the reasons for the increase in the reaction rates for the ions with the $D_{3/2}$ and $D_{5/2}$ states is the effect of the Li^++Ca(3d4s ^{3}D) level, which is close to the Li+Ca^+($D_{3/2}$, $D_{5/2}$) level. These levels can possibly cross at sufficiently short distances between the atom and ion, where the molecular potentials are significantly modified by the atom-ion interaction and strong core-repulsion [20, 22]. A detailed understanding of the charge exchange collision coefficients in our system requires the related energy levels to be further studied.

Despite in an extremely low production rate, the molecular ion formation has been observed several times in our system. Figure 4(b) shows the ion images before (top panel) and after atom-ion interaction. An extinction of the ion fluorescence due to inelastic collisions can be observed, but this is caused by the replacement of one of the ions with the dark ion, which shows clear contrast to the result shown in Figure 1(a,b). During the measurement process, an experimental condition of q_{Li^+}=1.2 is chosen; therefore, it is unlikely that the product ion is Li^+. We assume that the dark ion is a $CaLi^+$ molecule ion, but since the probability of this event is extremely low (less than 0.1 % of the charge exchange collisions), the mass spectrometry of the molecular ion has not been successfully conducted. Determining the molecule ion mass and specifying the molecule formation path will be objectives of a future study.

In conclusion, we have created an ultracold mixture of laser-cooled $^{40}Ca^+$ ions and fermionic ^{6}Li atoms. An atom-ion inelastic collision is observed in the hybrid system and it is concluded that the inelastic collision is a charge exchange process by identifying the reaction product as Li^+ ions via mass spectrometry. The charge exchange collision cross sections are also measured. The ion loss from the atom-ion inelastic collisions is largely suppressed for the ions in the electronic ground state, which is advantageous for the sympathetic cooling of Ca^+ ions when attempting to reach a micro-Kelvin regime without a significant loss of ions. Simultaneously, the reaction rate can be dynamically switched by applying a short optical pulse to excite the ions to the metastable states. This capability of on-off switching can be useful to control ultracold chemical reactions and for the application of ions as a high-spatial resolution probe of atomic gases in an optical lattice potential.

[1] D. J. Heinzen, R. Wynar, P. D. Drummond and K.V. Kheruntsyan, Phys. Rev. Lett. **84**, 5029 (2000).

[2] K. Ravi, S. Lee, A. Sharma, G. Werth and S. Rangwala, Nature comm. **3**, 1126 (2012).

[3] A. Grier, M. Cetina, F. Oručević, and V. Vuletić, Phys. Rev. Lett. 102, 223201 (2009).

[4] C. Zipkes, S. Palzer, C. Sias and M. Kohl, Nature **464** 388 (2010).

[5] S. Schmid, A. Härter, and J. H. Denschlag, Phys. Rev. Lett. **105**, 133202 (2010).

[6] W. Rellergert, S. Sullivan, S. Kotochigova, A. Petrov, K. Chen, S. Schowalter and E. Hudson, Phys. Rev. Lett. **107**, 243201 (2011).

[7] L. Ratschbacher, C. Zipkes, C. Sias, and M. Köhl, Nature Phys. **8**, 649 (2012).

[8] Y. -P. Chang, K. Dlugolecki, J. Kupper, D. Rosch, D. Wild, S. Willitsch, Science **342**, 98 (2013).

[9] S. Haze, S. Hata, M. Fujinaga, and T. Mukaiyama, Phys. Rev. A **87**, 052715 (2013).

[10] Y. Sherkunov, B. Muzykantskii, N. d'Ambrumenil and B. D. Simons, Phys. Rev. A **79**, 023604 (2009).

[11] F. Cucchietti and E. Timmermans, Phys. Rev. Lett. **96**. 210401 (2006).

[12] M. Cetina, A. Grier and V. Vuletić, Phys. Rev. Lett. **109**, 253201 (2012).

[13] A. Mosk, S. Jochim, H. Moritz, Th. Elsasser, M. Wei-

demuller, and R. Grimm, Opt. Lett. **26**, 1837 (2001).
[14] Y. Inada, M. Horikoshi, S. Nakajima, M. Kuwata-Gonokami, M. Ueda and T. Mukaiyama, Phys. Rev. Lett. **101**, 180406 (2008).
[15] The average atomic density is determined from $n_{\rm a} = \int n_{\rm atom}(\mathbf{r}) n_{\rm ion}(\mathbf{r}) d\mathbf{r}$, where $n_{\rm atom}(\mathbf{r})$ and $n_{\rm ion}(\mathbf{r})$ are the density profiles determined from the trap frequencies and temperatures of the atoms and ions.
[16] A. Kreuter, C. Becher, G. P. T. Lancaster, A. B. Mundt, C. Russo, H. Haffner, C. Roos, W. Hansel, F. Schmidt-Kaler, R. Blatt, M. S. Safronova, Phys. Rev. A **71**, 032504 (2005).
[17] P. Langevin, Ann. Chim. Phys. **5**, 245 (1905).
[18] D. Leibfried, R. Blatt and D. Wineland, Rev. Mod. Phys. **75**, 281 (2003).
[19] C. Zipkes, S. Palzer, L. Ratschbacher, C. Sias, and M. Köhl, Phys. Rev. Lett. **105**, 133201 (2010).
[20] F. Hall, M. Aymar, N. Bouloufa-Maafa, O. Dulieu and S. Willitsch, Phys. Rev. Lett. **107**, 243202 (2011).
[21] B. Roth, P. Blythe, and S. Schiller, Phys. Rev. A **75**, 023402 (2007).
[22] E. Sayfutyarova, A. Buchachenko, S. Yakovleva, and A. Belyaev, Phys. Rev. A **87**, 052717 (2013).